Available online at www.sciencedirect.com
ScienceDirect
Materials Chemistry and Physics 109 (2008) 465–468
MATERIALS CHEMISTRY AND PHYSICS
www.elsevier.com/locate/matchemphys

Electrical relaxation in the compound: $LiFeVO_4$

Moti Ram

Department of Physics and Meteorology, Indian Institute of Technology Kharagpur, Kharagpur, West Bengal 721302, India

Received 20 August 2007; received in revised form 10 December 2007; accepted 15 December 2007

Abstract

Layered ceramic oxide ($LiFeVO_4$) has been prepared by a standard solid-state reaction technique. $LiFeVO_4$ has orthorhombic crystal structure whose dielectric and electrical modulus properties were studied over a range of frequency (100 Hz–1 MHz) and temperature (298–598 K) using complex impedance spectroscopy (CIS) technique. Dielectric results suggest dielectric relaxation in the material. The presence of non-Debye type conductivity relaxation in the material has been confirmed by complex electrical modulus analysis. The activation energy calculated from electric modulus spectra is 0.237 ± 0.005 eV.

Keywords: Ceramics; Sintering; Electrical properties

1. Introduction

The concept of dielectric relaxation is associated with ionic/electronic conductivity in layered ceramic oxides under the influence of ac field. Our study is concerned with frequency dependence of ac electrical properties and associated relaxation phenomena of layered ceramic oxides. Layered ceramic oxides having spinel or bronze structure [1,2] have been found useful for energy storage applications (such as in batteries, capacitors, fuel cells, etc.) and quite a number of them have also been commercialized, they are yet to fulfill the cherished commercial goal [3,4]. Vanadium-based oxides having layered structure appear as better alternative because they satisfying requirements of stable phase, environmental friendliness, cost effectiveness and better performance [5]. Analyses of dielectric properties of ceramics are important to investigate the nature of barrier properties for applications in devices. In recent times, olivine structure type ceramic oxides are potential materials for electrochemical applications in the devices as electrodes because of their layered structure and voids in them matching with the dimensions of alkali metal ions, i.e., Li^+, Na^+, etc. Iron-based ceramic oxides become a natural choice due to their layered structure, direct Fe–Fe or Fe–O–Fe linkage arising from an edge shared octahedral arrangement and presence of a corrugated layer of appropriate dimension (∼2 Å). However, literature shows electrochemical performance of such oxides, e.g., α-$NaFeO_2$ and $LiFeO_2$ [6–8] is poor due to low electronic conductivity of the material. Electrochemical devices require good ionic mobility as well as reasonable electronic conduction. The interfacial impedance should be low with practically very little barrier to charge transfer. In this paper, I report dielectric and electrical modulus properties of the vanadium-based layered ceramic oxide ($LiFeVO_4$) having bulk (measured) density 3.072 g cm^{-3}.

2. Experimental procedures

Highly purity (AR grade) precursors (Li_2CO_3, Fe_2O_3, V_2O_5) were weighed and taken in appropriate stoichiometric ratio. The physical mixture was then mixed mechanically prior to being put in a furnace. Solid-state reaction was carried out in air atmosphere at a temperature of 570 °C for 8 h. The calcinations temperature has been optimized using thermal analysis (DTA/TGA) technique prior to calcination. Materials formation was confirmed by X-ray diffraction (XRD) studies. XRD pattern of the material sample was recorded at room temperature using a diffractometer (Rigaku, model: Mini Flex) in the range of Bragg angle ($20^\circ \leq 2\theta \leq 80^\circ$) on being irradiated by Cu Kα (1.5405 Å). The calcined powder was pelletized into disk type pellets of diameter (10–11 mm) and various thicknesses (1–3 mm) with polyvinyl alcohol (PVA) as binder using hydraulic press under a pressure of ∼2–3 tonnes. These pellets were then sintered at 550 °C for 5 h followed by a slow cooling process. Subsequently, the pellets were polished by fine emery paper to make their faces smooth and parallel. The pellets were finally coated with conductive silver paint and dried at 150 °C for ∼2–3 h before carrying out electrical measurements. Electrical measurements were done at an input ac signal of voltage amplitude ∼1.2 V over a range of frequency (100 Hz–1 MHz) and temperature range (298–598 K) using a computer-controlled frequency response analyzer (HIOKI LCR HI Tester, Model: 3532).

E-mail address: motiram05@yahoo.co.in.

0254-0584/$ – see front matter © 2007 Elsevier B.V. All rights reserved.
doi:10.1016/j.matchemphys.2007.12.020

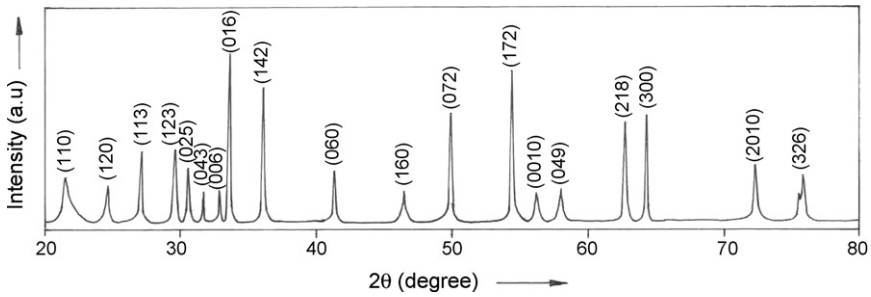

Fig. 1. X-ray diffraction pattern of $LiFeVO_4$ at room temperature.

3. Results and discussion

3.1. Structural analysis

X-ray diffraction pattern of calcined powder of the compound at room temperature is shown in Fig. 1, which confirms the formation of the material sample ($LiFeVO_4$) under the reported conditions. The X-ray diffractogram comprises of sharp diffraction peaks of varying intensity. The peaks have been indexed using standard computer software (POWDMULT) [9]. XRD analysis reveals an orthorhombic unit cell structure of the investigated compound. The lattice parameters as evaluated using the software were refined by a least squares fitting technique, which are $a = 4.3368$ (26) (Å), $b = 13.1119$ (26) (Å), and $c = 16.3426$ (26) (Å). The average crystallite size of compound was found to be ~50.34 nm using Scherer's equation $P = k\lambda/\beta_{1/2}\cos\theta_{hkl}$, where $k = 0.89$, $\lambda = 1.5405$ Å, and $\beta_{1/2}$ = half peak-width [10]. More details on structural analysis can be found in Ref. [11].

3.2. Dielectric analysis

Dielectric properties of the system have been studied over a range of frequency and temperature. Fig. 2 shows the variation of dielectric constant (ε_r) as a function of frequency at different temperatures. These graphs indicate a dispersive behavior at low frequencies, reflecting blocking effects. Dispersive behavior in the dielectric constant is due to two sources: (i) polarized structure of studied material and (ii) associated with mobile charge carriers [12]. The high value of ε_r at low frequency for all temperatures is due to presence of all types polarizations viz electronic, dipolar, interfacial and ionic orientation, etc. Further, ε_r decreases with increasing frequency. These are typical characteristic of dielectric material [13,14].

The variation of dielectric loss ($\tan\delta$) as a function of the frequency at different temperatures has been represented in Fig. 3. The value of $\tan\delta$ deceases gradually with increasing frequency up to 200 °C. The $\tan\delta$ peaks of dielectric relaxation were observed at temperatures (≥250 °C) and shift towards the higher frequency region with decease in the value of $\tan\delta$. This type of feature suggests the presence of dielectric relaxation in the compound [14,15].

Fig. 4 represents the variation of dielectric constant (ε_r) and dielectric loss as a function of temperature at 1 kHz. Initially, the value of ε_r and $\tan\delta$ increases with increasing temperature at given frequency. The presence of the $\tan\delta$ peak at the temperature $T_m = 538$ K with $\tan\delta_m = 6.47$ suggests dielectric relaxation in the material [14,15].

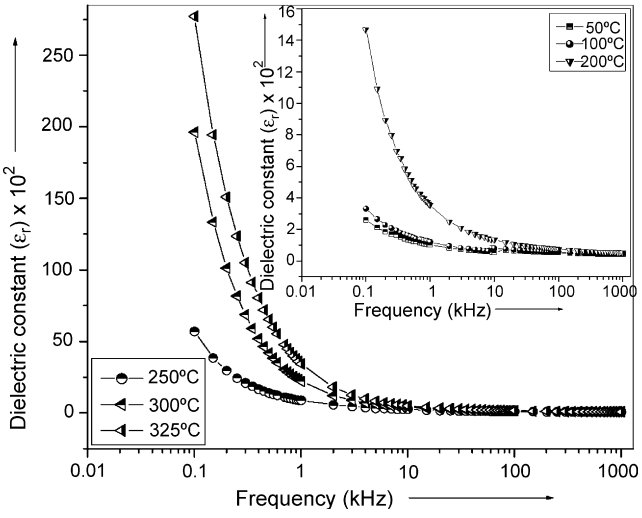

Fig. 2. Variation of dielectric constant (ε_r) as a function of frequency at different temperatures.

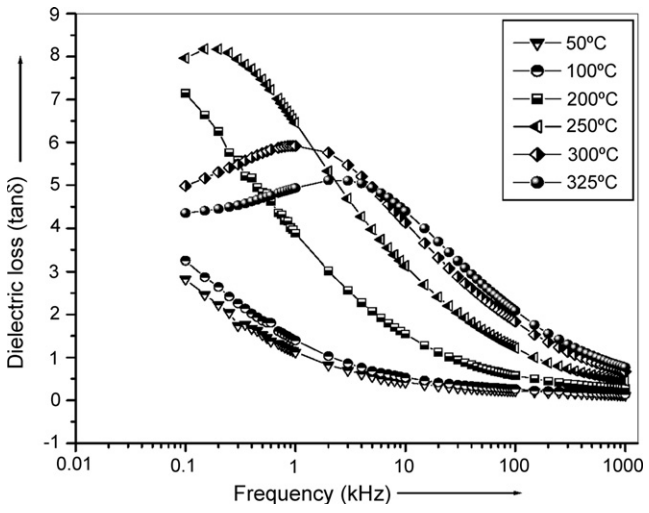

Fig. 3. Variation of dielectric loss ($\tan\delta$) as a function of frequency at different temperatures.

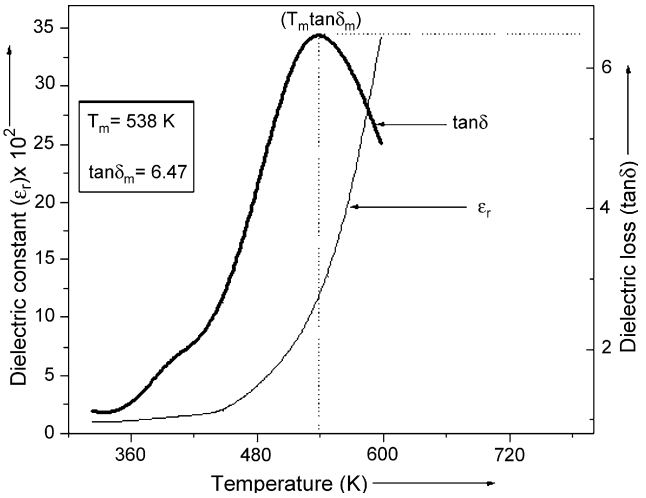

Fig. 4. Variation of dielectric constant (ε_r) and dielectric loss (tan δ) as a function of temperature at 1 kHz.

3.3. Electrical modulus analysis

The complex modulus spectrum indicates electrical phenomenon with the smallest capacitance occurring in the material sample. Fig. 5 represents the complex modulus spectrum of the material sample at different temperatures. The appearance a single semicircular arc in the pattern at different temperatures confirms the presence of electrical relaxation phenomena and the single-phase character of $LiFeVO_4$ which is good agreement with the results of XRD analysis.

Fig. 6 shows variation of real part of electric modulus as a function of frequency at different temperatures. In fact M' reaches a maximum constant value $M_\infty = 1/\varepsilon_\infty$ at higher frequencies and approaches zero at low frequencies. These features indicate that the electrode polarization makes a negligible contribution in the material [16]. M' levels off at higher frequencies and temperatures due the spread of relaxation processes over a range of frequencies.

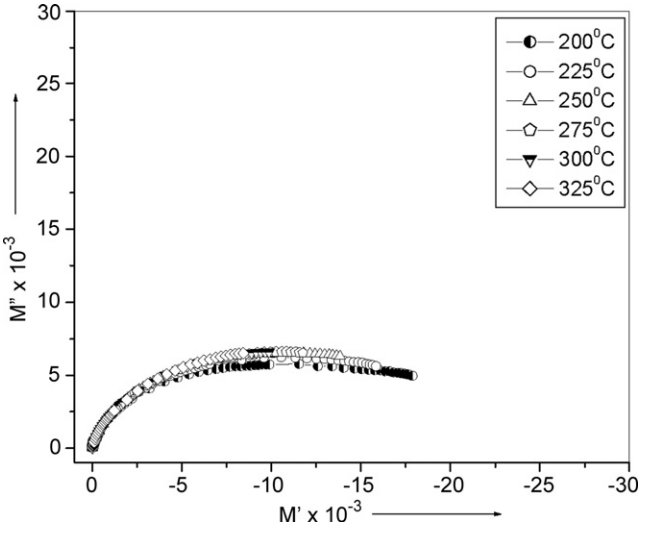

Fig. 5. Complex modulus spectrum of material sample at different temperatures.

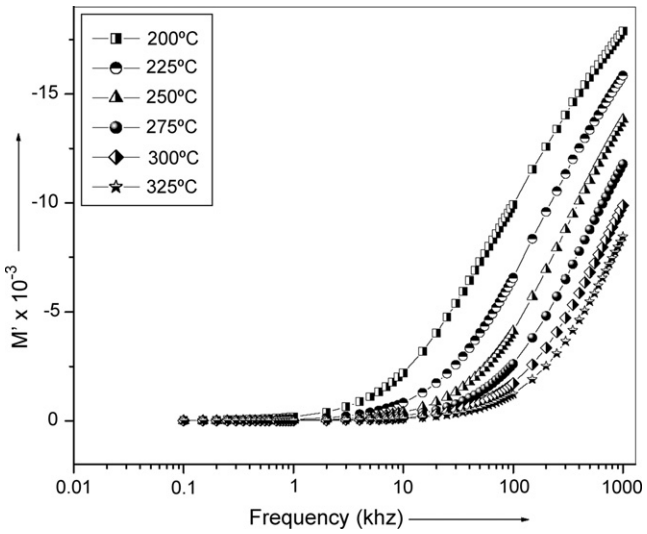

Fig. 6. Variation of real part of electrical modulus as a function of frequency at different temperatures.

Fig. 7 shows the variation of imaginary part of electric modulus as a function of frequency at different temperature and it centered at dispersion region of M'. It is characterized by: (i) presence of modulus peaks in the pattern, (ii) significant asymmetry in the peak with their positions lying in the dispersion region of M' versus frequency pattern (Fig. 6) and (iii) the modulus peak position shift towards higher frequency side with increasing temperature. The frequency f_{max} (corresponding to M''_{max}) gives the most probable conduction relaxation time (τ_σ) from the condition $2\pi f_{max} = 1$ and its variation as a function of temperature is shown in Fig. 8. This plot obeys the Arrhenius' relation:

$$\tau_\sigma = \tau_{\sigma_0} \exp\left[-\frac{E_a}{kT}\right] \quad (1)$$

where $\tau_{\sigma 0}$ is a pre-exponential factor, E_a is the activation energy, k is the Boltzmann constant and T is the absolute temperature

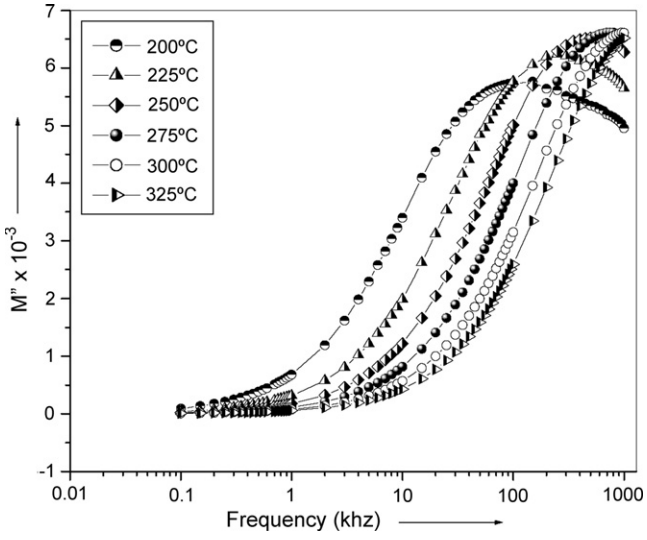

Fig. 7. Variation of imaginary part of electrical modulus as a function of frequency at different temperatures.

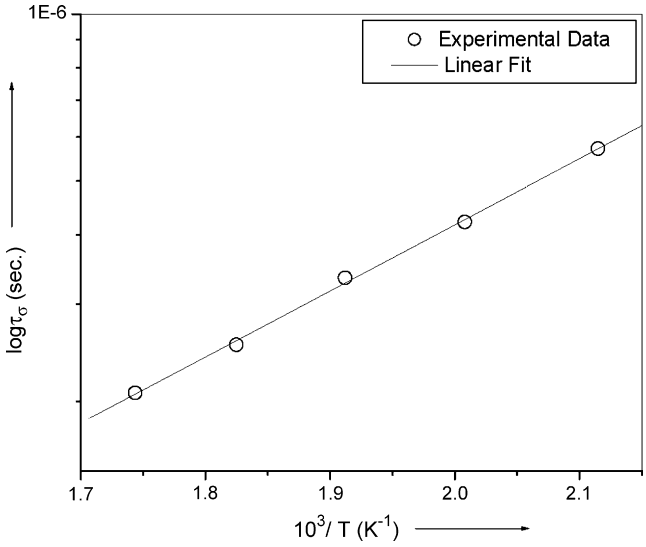

Fig. 8. Variation of relaxation time (τ_σ) as a function of temperature.

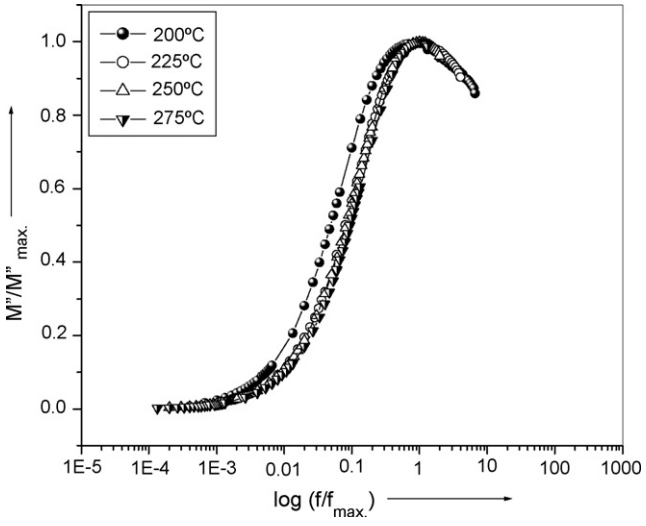

Fig. 9. Modulus master curve of $LiFeVO_4$.

[17,18]. The activation energy (E_a) calculated from linear fit to the data points is 0.237 ± 0.005 eV. Also, the appearance of peak in the pattern indicates the presence of conductivity relaxation in the compound.

The modulus master curve of $LiFeVO_4$ is given in Fig. 9. It shows the scaling behavior of the sample electrical modulus. The modulus master curve is characterized by (i) broad asymmetric pattern with a cross over from short-range mobility to long-range mobility of ions with rise in temperatures; (ii) more or less the same shape and pattern with slight variation in full width at half maximum (FWHM) with rise in temperature; (iii) FWHM is greater than the width of a typical Debye peak (1.14 decade). These observations indicate the presence of dynamical processes within the sample at different frequencies with same thermal activation energy and are independent of temperature with non-Debye type of conductivity relaxation. This suggests that the ion migration takes place via hopping mechanism [19,20].

4. Conclusions

The present work reports the results of our investigation on the dielectric and electrical modulus properties of the compound $LiFeVO_4$. XRD studies reveal an orthorhombic unit cell structure at room temperature with lattice parameters: $a = 4.3368$ (26) (Å), $b = 13.1119$ (26) (Å), and $c = 16.3426$ (26) (Å). Dielectric analyses suggest dielectric relaxation in the material. Modulus analysis indicates non-Debye type conductivity relaxation in the material. The activation energy (E_a) calculated from electric modulus spectra is 0.237 ± 0.005 eV.

Acknowledgement

The author is grateful to the Ferroelectrics Laboratory, Department of Physics & Meteorology and Central Research Facility, Indian Institute of Technology, Kharagpur 721302, West Bengal, India for providing research facilities.

References

[1] B. Domenges, M. Hervieu, B. Raveau, M. O' Keeffe, J. Solid State Chem. 72 (1988) 155–172.
[2] J.M. Haussonne, G. Desgardin, A. Herve, B. Boufrou, J. Eur. Ceram. Soc. 10 (1992) 437–452.
[3] H.A. Kiehne (Ed.), Battery Technology Handbook, 2nd edition, Marcel Dekker Inc., New York, 2003.
[4] D.A.J. Rand, R. Woods, R.M. Dell, Batteries for Electric Vehicles, John Wiley & Sons Inc., New York, 1998.
[5] G.B. Appetecchi, F. Croce, M. Mastragostino, B. Scrosati, F. Soavi, A. Zanelli, J. Electrochem. Soc. 145 (1998) 4133–4135.
[6] B. Fuchs, S. Kemmler-Sack, Solid State Ionics 68 (1994) 279–285.
[7] M. Tabuchi, K. Ado, H. Sakaebe, Solid State Ionics 79 (1995) 220–226.
[8] K. Ado, M. Tabuchi, H. Kobayashi, H. Kageyama, O. Nakamura, Y. Inaba, R. Kanno, M. Takagi, Y. Takeda, J. Electrochem. Soc. 144 (1997) L117–L180.
[9] E. Wu, POWDMULT: An Interactive Powder Diffraction Data Interpretation and Indexing Program, Version 2.1, School of Physical Sciences, Flinder University of South Australia, Bardford Park, SA, Australia, 1989.
[10] H.P. Klug, L.B. Alexander, X-ray Diffraction Procedures, Wiley, New York, 1974.
[11] M. Ram, R.N.P. Choudhary, A.K. Thakur, Adv. Appl. Ceram. 105 (2006) 140–147.
[12] L. Bucio, E. Orozco, A. Huanosta-Tera, J. Phys. Chem. Sol. 67 (2006) 651–658.
[13] M.E. Lines, A.M. Glass, Prin. and Appl. of Ferroelectrics, Oxford University Press, Oxford, UK, 1977.
[14] N.K. Singh, A. Panigrahi, R.N.P. Choudhary, Mater. Lett. 50 (2001) 1–5.
[15] B. Tareev, Physics of Dielectric Materials, Mir Publishers, Moscow, 1979.
[16] B.V.R. Chowdari, R. Gopalkrishnan, Solid State Ionics 23 (1987) 225–233.
[17] S. Sen, P. Pramanik, R.N.P. Choudhary, Appl. Phys. A: Mater. Sci. Process. 82 (2006) 549–557.
[18] J.-M. Reau, A. Simon, M. El Omari, J. Ravez, J. Eur. Ceram. Soc. 19 (1999) 777–779.
[19] K.P. Padmasree, D.K. Kanchan, A.R. Kulkarni, Solid State Ionics 177 (2006) 475–482.
[20] M. Dong, J.-M. Reau, J. Ravez, Solid State Ionics 91 (1996) 183–190.